available at www.sciencedirect.com

SCIENCE DIRECT®

journal homepage: www.elsevier.com/locate/biochempharm

Cytotoxic efficacy of an anthraquinone linked platinum anticancer drug

R.A. Alderden [a], H.R. Mellor [b], S. Modok [b], T.W. Hambley [a], R. Callaghan [b,*]

[a] Centre for Heavy Metals Research, School of Chemistry, The University of Sydney, NSW 2006, Australia
[b] Oxford Drug Resistance Group, Nuffield Department of Clinical Laboratory Sciences, John Radcliffe Hospital, University of Oxford, Oxford OX3 9DU, UK

ARTICLE INFO

Article history:
Received 2 December 2005
Accepted 20 December 2005

Keywords:
Platinum
Chemotherapy
Cancer
Lysosomes
Anthraquinone
Cytotoxicity

ABSTRACT

Platinum complexes are widely used in cancer chemotherapy; however, they are associated with toxicity, high ''non-specific'' reactivity and relatively poor pharmacokinetic profiles. In particular, their low cellular uptake and rapid metabolic inactivation means that the amount of ''active'' drug reaching the nuclear compartment is low. Our strategy to facilitate nuclear accumulation was to introduce a hydrophobic anthraquinone (1C3) moiety to the Pt-complex. Anthraquinones are known to readily intercalate into DNA strands and hence, the Pt-1C3 complex may represent an effective system for the delivery of the platinum moiety to nuclear DNA. Efficacy of the complex was determined by measuring the extent and potency of cytotoxicity in comparison to cisplatin and an anthraquinone based anticancer drug, doxorubicin. The Pt-1C3 complex generated higher levels of cytotoxicity than cisplatin, with a potency of 19 ± 4 μM in the DLD-1 cancer cell line. However, this potency was not significantly different to that of the 1C3 moiety alone. To examine the reason for the apparent lack of platinum related cytotoxicity, the cellular distribution was characterised. Confocal fluorescence microscopy indicated that the Pt-1C3 complex was rapidly sequestered into lysosomes, in contrast to the nuclear localisation of doxorubicin. In addition, there was negligible DNA associated Pt following administration of the novel complex. Thus, the addition of a 1C3 moiety generated sequestration of the complex to lysosomes, thereby preventing localisation to the nucleus.

1. Introduction

Cisplatin is used for the treatment or palliation of many types of cancer including non-small cell lung, ovarian and testicular [1]. However, these cancers frequently develop resistance to cisplatin and many others display an inherent lack of sensitivity. The limited effectiveness of cisplatin is due to many factors including: (a) a poor pharmacokinetic profile, (b) low accumulation in cells, (c) increased production of intracellular thiols (e.g. glutathione and metallothionein) and (d) increased DNA repair capacity [2–4]. Investigations outlining these cellular effects have shed considerable light on the mechanisms of anticancer drug resistance and considerable effort has been directed towards the development of novel platinum containing compounds that deliver greater efficacy.

Often, strategies aimed at improving platinum drug efficacy attempt to increase cellular uptake and facilitate targeting of the compounds to DNA [5,6]. The latter involves the incorporation of a functional group into the platinum complex that will interact or intercalate with DNA. Additional benefits of this intercalation strategy include a reduction in

* *Corresponding author*. Tel.: +44 1865 221 110; fax: +44 1865 221 834.
E-mail address: richard.callaghan@ndcls.ox.ac.uk (R. Callaghan).
0006-2952/$ – see front matter © 2006 Elsevier Inc. All rights reserved.
doi:10.1016/j.bcp.2005.12.039

non-specific modification of cellular macromolecules and the possible generation of novel DNA lesions. The latter may evade DNA repair processes leading to more effective disruption of DNA replication. For example, diaminocyclohexane–Pt–DNA adducts generated by oxaliplatin can trigger apoptosis more efficiently than diammine–Pt–DNA adducts produced by cisplatin in certain tumour types [7]. Furthermore, a number of Pt-complexes containing the DNA intercalating agent 9-aminoacridine have been developed and these compounds display increased reaction with DNA with a novel reaction mechanism to generate the adduct [8].

The structure activity relationships and antitumour activity of several platinum complexes linked to anthraquinone intercalating moieties by an alkyl amino chain have been examined [9–13]. A number of these complexes were shown to have equivalent in vitro and in vivo activity to cisplatin and to possess higher activity than the components individually (the free anthraquinone ligand and the analogous platinum complex) or a 1:1 molar mixture of the two [11].

Alkylamino-anthraquinone containing compounds such as the anthracycline antibiotic doxorubicin are established and clinically used anticancer drugs. Doxorubicin is known to intercalate into DNA and this observation sparked the development of novel DNA intercalators. For example, the clinically used anticancer drug mitoxantrone was developed from rational design on data obtained from chemical screening of anthraquinone-based intercalating agents [14,15]. Mitoxantrone interacts with DNA in a sequence selective manner and its intercalation leads to cytotoxicity via inhibition of Topoisomerase II. The high affinity interaction with DNA is thought to be stabilised by the two cationic (at physiological pH) alkylamino side chains that form electrostatic interactions and hydrogen bonds with the DNA strand [16–18]. In addition, a systematic chemical screening investigation has identified the cationic alkylamino group on mitoxantrone derivatives as a key factor in the nuclear localisation, DNA binding and inhibition of DNA synthesis [19].

In the present study a novel Pt(II)-complex containing a co-ordinated alkylamino-anthraquinone compound was examined for its efficacy to produce cytotoxicity in a colon cancer cell line. The efficacy was compared to the anthraquinone ligand, cisplatin, a hydrophobic Pt-complex (JM118) and doxorubicin. The ability of the novel Pt–anthraquinone complex to generate cytotoxicity was related to its subcellular localisation.

2. Materials and methods

2.1. Materials

RPMI-1640 + Glutamax I culture medium, foetal bovine serum, trypsin–EDTA and penicillin/streptomycin were all purchased from Life Technologies—Invitrogen (Paisley, UK). Doxorubicin hydrochloride was obtained from Sigma Laboratories (Poole, UK). SYTO21, MitoTracker Green and LysoTracker Green were all purchased from Molecular Probes—Invitrogen. All solvents and reagents were of at least analytical grade and were used as received without further purification, unless otherwise stated.

2.2. Chemical synthesis of platinum complexes

2.2.1. Instrumentation

Diffuse reflectance infrared Fourier transform spectra (DRIFTS) were measured on a BIO-RAD FTS-40 or FTS-7 spectrophotometer. Potassium bromide was used as both the background and the matrix over the range 400–4000 cm^{-1}. ^{1}H and ^{13}C NMR spectra were recorded at 300 K on a Bruker AMX 300 MHz spectrometer. All spectra were recorded using commercially available solvents (Aldrich) of >99.6% isotopic purity and referenced to TPS (3-(trimethylsilyl)propionic acid) or solvent isotopic impurities. ^{195}Pt NMR spectra were recorded at 300 K on a Bruker AMX 400 MHz spectrometer. Chemical shifts were referenced to $Na_2[PtCl_6]$. Elemental analyses (C, H, N) were performed by the Microanalytical Service of the Australian National University, Canberra, ACT, or Chemical and Micro Analytical Services, Belmont, Vic.

2.2.2. 1-[(3-Aminopropyl)amino]-anthracene-9,10-dione (1C3)

The following synthetic procedure is based upon that outlined by Barasch et al. [20]. Propane-1,3-diamine (15 mL, 180 mmol) was added to a solution of 1-chloroanthraquinone (10 g, 41 mmol) in dry toluene (350 mL, dried over anhydrous Na_2SO_4) and refluxed for 18 h. The red suspension was evaporated to dryness under reduced pressure and resuspended in chloroform (500 mL). Gaseous hydrochloric acid was bubbled through the suspension for approximately 2 days, or until the mixture became pale pink in colour. The product was extracted into an aqueous layer with several washings of water. Using 3 M NaOH, the pH of the aqueous layer was adjusted to approximately 8, followed by subsequent extraction of the final product into chloroform. The solution was evaporated to dryness under reduced pressure, giving a red solid (7.6717 g, 27.4 mmol, 77% yield). ^{1}H NMR (300 MHz, $CDCl_3$) δ 9.74 (broad, 1H), 8.24 (m, 2H), 7.72 (m, 2H), 7.57 (dd, 1H), 7.51 (t, 1H), 7.07 (dd, 1H), 3.41 (m, 2H), 2.93 (t, 2H), 1.91 (m, 2H), 1.38 (broad, 2H); ^{13}C NMR (300 MHz, $CDCl_3$) δ 185.10, 183.89, 151.86, 135.41, 135.11, 134.75, 134.02, 133.13, 133.01, 126.81, 126.75, 117.94, 115.75, 113.06, 40.68, 39.94, 32.92; IR (KBr, cm^{-1}): 3356 m, 3273 m, 3182 m, 2934 m, 2862 m, 1662 s, 1628 s, 1594 s, 1572 s, 1511 s, 1470 m, 1465 m, 1409 m, 1303 s, 1272 s, 1236 m, 1176 m, 1160 m, 1071 m, 1019 m, 972 m, 916 m, 830 m, 806 m, 786 m, 735 s, 709 s, 673 m, 662 m, 598 m, 549 m, 481 m, 419 m.

2.2.3. Amminetrichloroplatinate(II) $[PtCl_3(NH_3)]^-$

The following synthetic procedure is based upon that outlined by Cai et al. [21]. Cisplatin (4.0 g, 13.3 mmol), tetraethylammonium chloride monohydrate (2.94 g, 16.0 mmol), and ammonium chloride (0.20 g, 3.7 mmol) were dissolved in *N*,*N*-dimethylacetamide (150 mL). The reaction mixture was heated at 100 °C, purging with a slow stream of N_2 for 8–10 h. The solution changed from yellow to orange in colour, and its volume evaporated to approximately 50 mL, during the course of the reaction. Hexane/ethyl acetate (1:1, 300 mL) was added to the solution and it was kept overnight at −20 °C. The supernatant was decanted off, and the solid extracted using 60 mL of acetonitrile. The remaining solid, assumed to be a mixture of ammonium chloride and cisplatin, was washed with water to recover unreacted cisplatin. Water (5 mL) was

added to the acetonitrile solution and the acetonitrile was removed under reduced pressure, resulting in an orange aqueous solution of $[PtCl_3(NH_3)]^-$ (11.58 mmol, 87% yield).

2.2.4. *cis-[1-[[(3-Aminopropyl)amino]-anthracene-9,10-dione]ammine]dichloro-platinum(II) (Pt-1C3)*

The following synthetic procedure is based upon that outlined by Gibson et al. [11]. A solution of 1C3 (1.6535 g, 5.9 mmol) in MeOH (approximately 2 L) was added to an aqueous solution of $[PtCl_3(NH_3)]^-$ (6.0 mmol) over a period of approximately 1 h. Additional MeOH was added, as required, to ensure that minimal precipitation occurred. The solution was stirred at room temperature for approximately 3 weeks, during which time a dark red precipitate formed. The solid was filtered and washed with MeOH. The resulting red solid was ground to a fine powder, resuspended in MeOH (500 mL), stirred for several days, then filtered and washed with MeOH. The process of resuspension was repeated until elemental analysis revealed that the product did not contain unreacted 1C3. The final product was obtained as a red solid (0.8309 g, 1.47 mmol, 25% yield). ^{195}Pt NMR (DMF/HCl): δ −2157 ppm. Analysis calculated for $PtC_{17}H_{19}N_3O_2Cl_2$: C, 36.25; H, 3.40; N, 7.46. Found: C, 36.37; H, 3.29; N, 7.32.

2.3. *DNA fluorescence titration*

Small quantities of a stock solution of calf thymus DNA were added to 38 μM solutions of 1C3 and Pt-1C3, such that the ratio of DNA base pairs:anthraquinone compound ranged from 0:1 to 8:1. Following each addition, solutions were mixed and fluorescence emission spectra recorded within 10 min.

2.4. *Cell culture*

The human colon adenocarcinoma cell line DLD-1 was kindly provided by Dr. Roger Phillips (University of Bradford, UK). The DLD-1 cells were grown in RPMI-1640 medium containing Glutamax I and 25 mM HEPES supplemented with 10% (v/v) heat inactivated foetal bovine serum and penicillin/streptomycin (100 IU/mL and 100 mg/mL, respectively). Cells were grown at 37 °C (5% CO_2) as monolayer cultures for a maximum of 20 passages and routinely harvested with trypsin–EDTA.

2.5. *Drug cytotoxicity assays*

DLD-1 cells were seeded in 96-well plates at a density of 3×10^3 cells per well in 100 μL supplemented medium. The cells were

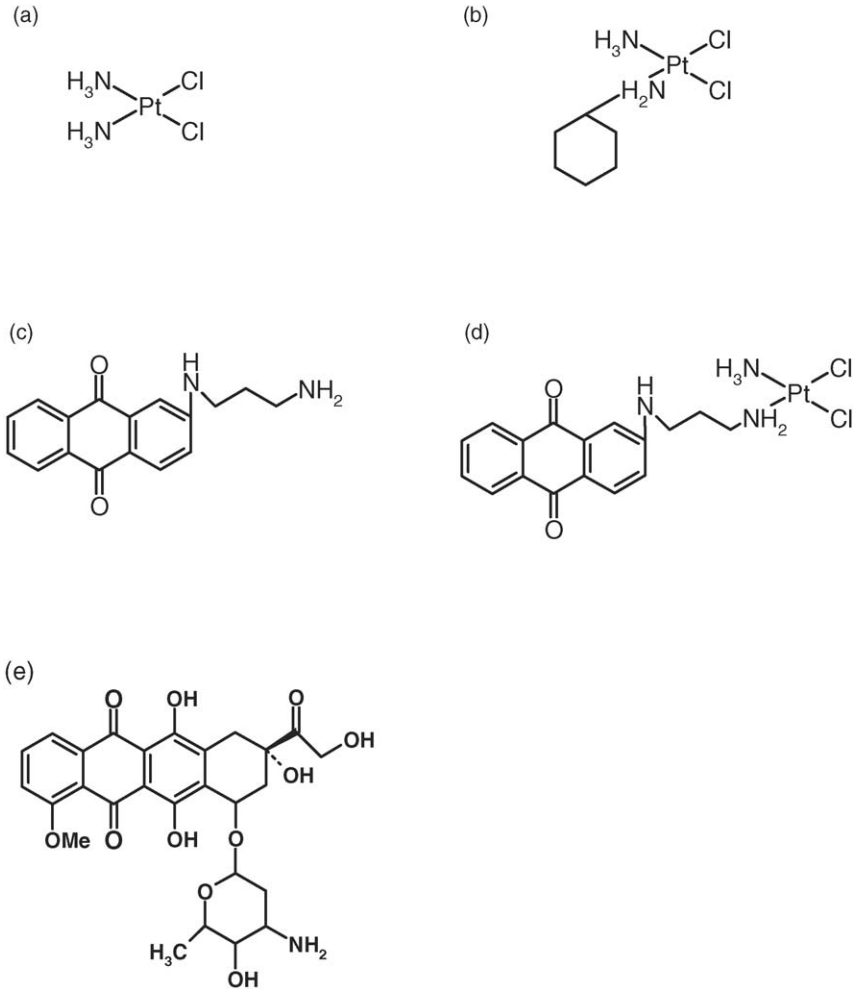

Fig. 1 – Structures of drugs used in the investigations. Structures of: (a) cisplatin, (b) JM118, (c) 1-[(3-aminopropyl)amino]-anthracene-9,10-dione (1C3), (d) *cis*-[1-[[(3-aminopropyl)amino]-anthracene-9,10-dione]ammine]dichloro-platinum(II) (Pt-1C3) and (e) doxorubicin.

allowed to adhere for 24 h prior to drug addition. Drugs were added in a 100 μL aliquot in culture medium at twice the desired final concentration. Stocks of cisplatin and JM118 were made at 0.5 mM in 100 mM KCl and added to cells in the concentration range 5×10^{-7} to 2×10^{-5} M. The relative insolubility of the platinum complex containing the anthraquinone moiety (Pt-1C3) and the organic moiety alone (1C3) precluded storage in 100 mM KCl. Stock solutions of 0.5 mM were made in 100 mM KCl and 60% (v/v) dimethylformamide (DMF). Administration of the solvent DMF to the cells was maintained below 1% (v/v). Doxorubicin was stored as a 50 mM stock in DMSO and addition of this solvent to cells was maintained at <0.1% (v/v) and final drug concentrations were in the range 5×10^{-9} to 2×10^{-5} M.

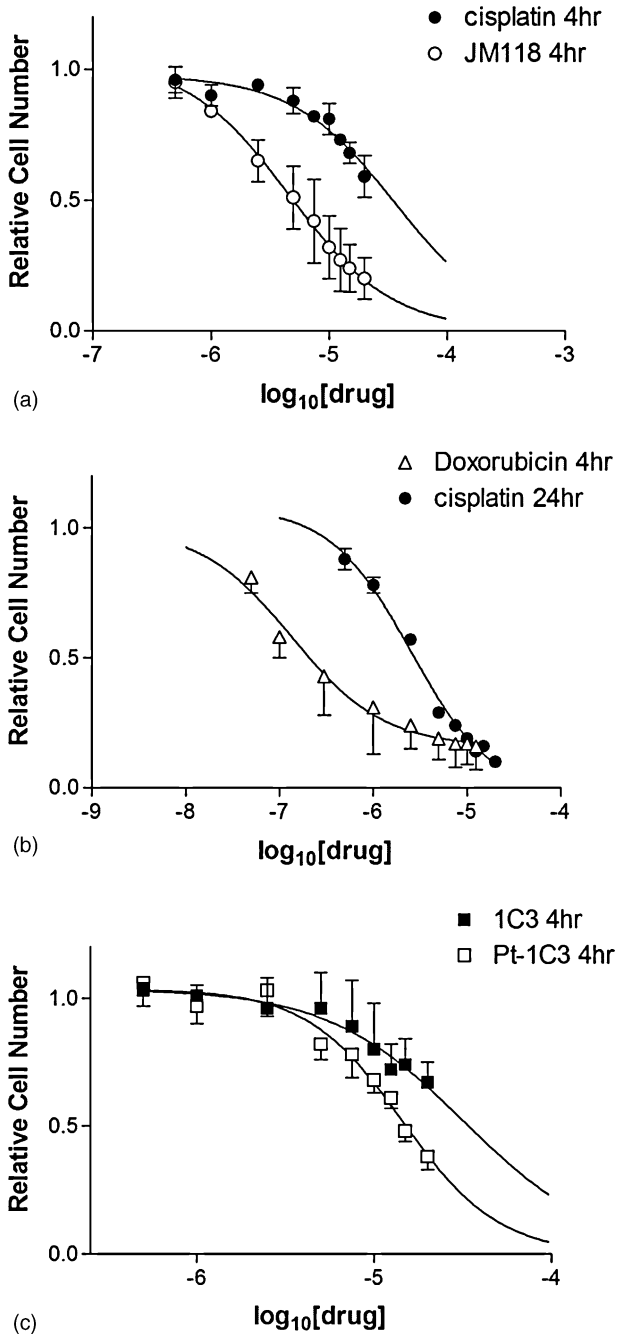

Fig. 2 – Drug induced cytotoxicity profiles. Dose-dependent cytotoxicity produced in DLD-1 cells cultured as monolayers exposed to the following: (a) cisplatin and JM118 for 4 h, (b) doxorubicin for 4 h and cisplatin for 24 h and (c) 1C3 and Pt-1C3, each for 4 h. The general dose–response equation was fitted using non-linear least squares regression and the data points represent mean ± S.E.M. of at least three independent observations. Cells remaining after the drug exposure and subsequent 72-h recovery period were determined using the MTT assay and the number in the absence of added drug was assigned a value of 1.0.

Cells were exposed to drugs for 2 or 4 h (unless otherwise indicated in figure legends) and then left for a "recovery" phase of 72 h in drug-free culture medium. Following "recovery", the number of viable cells was determined using the MTT assay. Absorbance (λ = 550 nm) was measured in a SpectraMAX 250 plate reader (Molecular Devices). Cell viability was plotted as a function of drug concentration and the cytotoxic potency (IC_{50}) estimated by non-linear regression of the general dose–response curve [22]. The viable cell number (cells remaining (% total)) was expressed as a percentage of the number obtained in the absence of drug treatment for the highest concentration of drug tested.

2.6. *Confocal fluorescence microscopy*

Monolayers were grown on coverslips in 6-well tissue culture plates to enable assessment of fluorescent drug and organelle specific probe localisation by confocal microscopy. Drugs (Pt-1C3 or 1C3) or probes were added from concentrated stocks directly to fresh culture medium and incubated at 37 °C for periods as indicated in the figure legends. The coverslips were then briefly washed in PBS and overlaid with 20% (v/v) glycerol

Table 1 – Cytotoxicity of platinum and anthraquinone containing compounds in the DLD-1 cell line

Drug	Exposure time (h)	Cells remaining (% total)	Potency (IC_{50}) (μM)
Cisplatin	2	77 ± 2	85 ± 19
	4	59 ± 8	34 ± 6
	24	10 ± 1	2.2 ± 0.3
Pt-1C3	2	38 ± 5	19 ± 4
	4	25 ± 7	11 ± 1
1C3	2	67 ± 8	25 ± 2
	4	48 ± 6	21 ± 6
JM118	2	29 ± 15	16 ± 7
	4	20 ± 8	5.9 ± 2.9
Doxorubicin	2	18 ± 9	0.30 ± 0.08
	4	16 ± 9	0.17 ± 0.04

DLD-1 cells were exposed to a range of drug concentrations over various exposure times and then allowed to recover for a further 72-h period. The number of cells remaining was measured with an MTT assay and plotted as a function of drug concentration. The percentage of cells remaining was determined at the maximal achievable drug concentration, which was 20 μM. The potency to generate cytotoxicity was estimated by non-linear regression analysis of the dose–response curve and all values represent the mean ± S.E.M. of at least three independent observations.

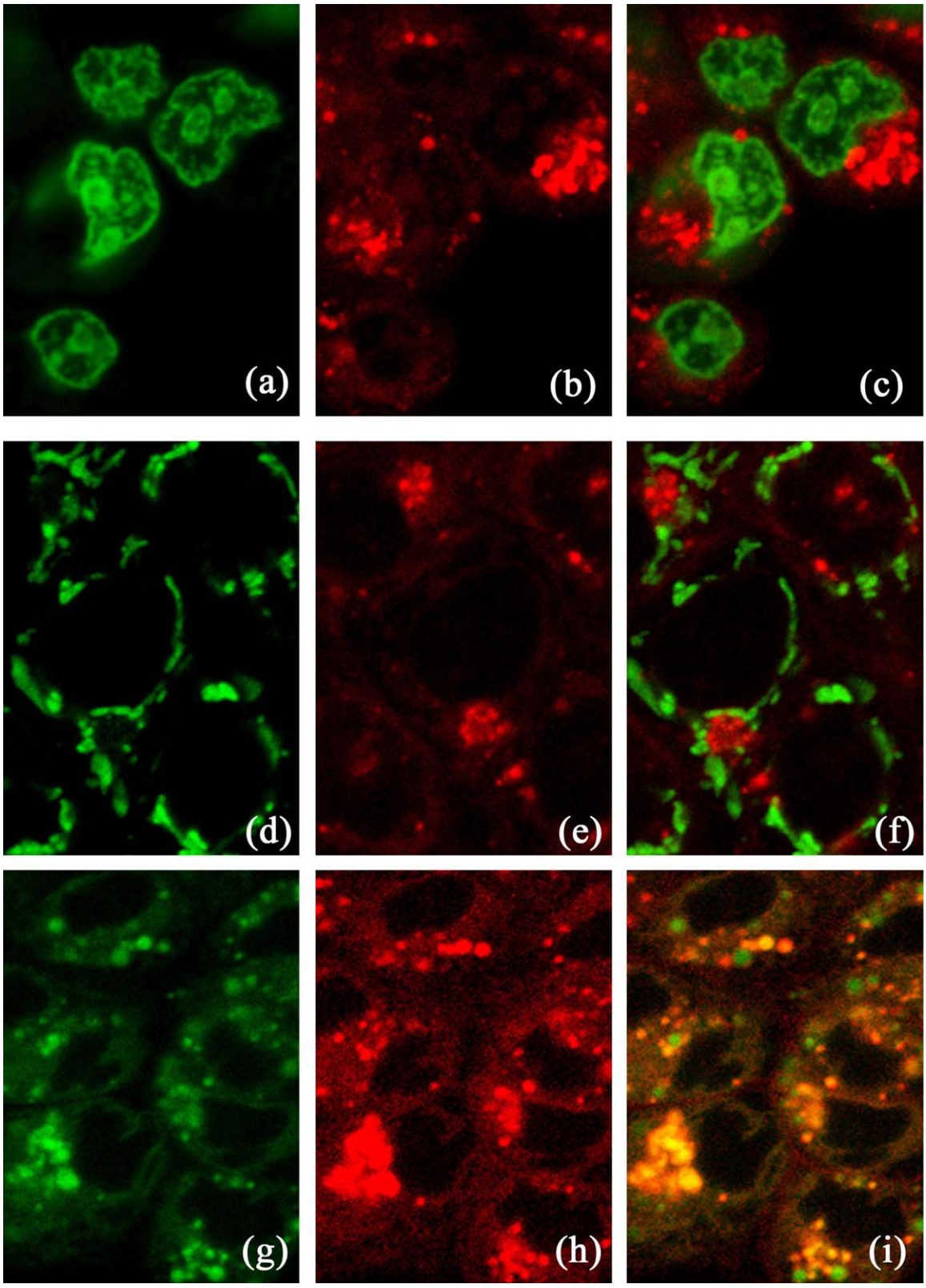

Fig. 3 – Cellular localisation of Pt-1C3. DLD-1 cells were grown to 80% confluency on glass coverslips in 6-well tissue culture plates and drugs were localised using confocal fluorescence microscopy. Panels (a–c) were obtained from cells incubated in the presence of Pt-1C3 (12 μM) for 4–5 h at 37 °C in the presence of the cell permeant nuclear stain SYTO21 (5 μM, 2 h, 37 °C). Panel (a) highlights localisation of the nuclear stain (λ_{ex} = 488 nm, 10–15% laser strength, λ_{em} = 505–530 nm). Panel (b) highlights localisation of Pt-1C3 (λ_{ex} = 543 nm, 76% laser strength, λ_{em} > 560 nm). Panel (c) is the overlay of panels (a and b). Panels (d–f) were obtained from cells incubated in the presence of Pt-1C3 (12 μM) for 4–5 h at 37 °C in the presence of the mitochondrial stain MitoTracker Green (0.2 μM, 30 min, 37 °C). Panel (d) highlights localisation of the mitochondrial stain

in PBS. Inverted coverslips were then placed on microscope slides and the edges sealed with clear nail varnish.

The fluorescent compounds were detected using a Zeiss LSM510 confocal laser scanning microscope (Carl Zeiss, Welwyn Garden City, UK). SYTO21 (nuclear stain), MitoTracker (mitochondrial stain) and LysoTracker (lysosomal stain) were all excited with an Argon laser at $\lambda = 488$ nm and detected using an emission filter set at $\lambda = 505$–530 nm. Doxorubicin, Pt-1C3 and 1C3 were all excited at $\lambda = 543$ nm with an emission filter set for $\lambda > 560$ nm.

2.7. Statistical and regression analyses

A minimum data set was obtained from at least three independent observations and values were expressed as mean ± S.E.M. Statistical comparisons of mean values were achieved using one-way ANOVA with Bonferroni's multiple comparison test and a P value < 0.05 was considered significant. All non-linear regression analyses were generated using the GraphPad Prism3.0 program.

3. Results

3.1. Cytotoxicity of doxorubicin and the Pt-complexes

The compounds used in this study are shown in Fig. 1. JM118 is considerably more hydrophobic than cisplatin based on the previously reported log P values [23]. The platinum complex containing an anthraquinone moiety is designated Pt-1C3 and the hydrophobic organic group is attached to the platinum via a short diaminoalkyl bridge. The anthraquinone molecule containing the diaminoalkyl chain is designated 1C3. The hydrophobic Pt-1C3 and 1C3 complexes are only sparingly soluble in aqueous buffer and therefore, the solvent DMF was used in the stock solutions. Initial examination of cytotoxicity used a procedure described previously [24], which involved a 72-h exposure of cells to a series of slow-acting Pt(IV)-complexes. However, DMF produced necrotic cell damage during this prolonged exposure. This toxicity was time-dependent since exposure of DLD-1 cells to DMF (0.05–2%, v/v) for periods up to 12 h did not generate any cytotoxic effect (data not shown). However, longer exposures produced a time-dependent toxicity. As a consequence, the DMF concentrations were maintained below 1% (v/v) and cells were exposed for a maximum of 4 h. Short exposure times represent a more realistic pharmacokinetic scenario. Cisplatin and JM118 were sufficiently soluble in 100 mM KCl buffer to alleviate the need for added solvent.

The DLD-1 cell line was used for a variety of reasons, in particular since the efficacy of a number of novel platinum chemotherapeutic agents have been examined using it. Furthermore, oxaliplatin is used as a first line treatment for advanced colorectal cancer. Thus it was thought that investigation of novel platinum compounds in colon cancer cell lines was relevant. The DLD-1 cells express Bcl2, a mutated version of p53 (Ser241Phe) and are considered MMR deficient. These features can potentially decrease the efficacy of platinum compounds, however, previously we have extensively characterised this cell line and it was sensitive to cisplatin ($IC_{50} = 14$ μM).

Fig. 2 shows examples of dose–response curves obtained for the various platinum complexes and doxorubicin in the treated DLD-1 cells. A 2-h exposure to cisplatin was associated with a viable cell count of 77 ± 2% at the highest dose used (20 μM). Extrapolation of the curve estimated that cisplatin displayed a potency of 85 ± 19 μM. However, increasing the exposure time to 24 h resulted in cytotoxicity in 90% of the cell population at the same concentration (i.e. 20 μM) and a significantly greater potency of 2.2 ± 0.3 μM (Fig. 2b and Table 1). In contrast, a 4-h exposure to the hydrophobic cisplatin derivative, JM118, was sufficient to generate cytotoxicity in 80% of the DLD-1 cells at 20 μM. The cytotoxic potency of a 4-h exposure of cells to JM118 was 5.9 ± 2.9 μM (Fig. 2a and Table 1). Presumably this difference in efficacy, particularly in a temporal manner, relates to the greater extent and rate of JM118 accumulation in cells, compared with the more hydrophilic cisplatin.

Doxorubicin is a widely used anthracycline class chemotherapeutic agent that displays significant hydrophobicity. The hydrophobicity is due to an anthraquinone moiety and the cytotoxicity of doxorubicin is due to inhibition of Topoisomerase II activity. A 4-h exposure to DLD-1 cells produced significant cytotoxicity as evident by the viable cell population of less than 20% (Fig. 2). The potency of doxorubicin for a 4-h exposure was 0.17 ± 0.04 μM and similar effects were observed for a 2-h exposure (Table 1). Clearly this compound displays a rapid and extensive intracellular accumulation in the DLD-1 colon cancer cell line.

Could the incorporation of a hydrophobic anthraquinone moiety into a platinum complex also facilitate uptake into cells and achieve greater efficacy in eliciting cytotoxicity? Fig. 2c shows the dose response curve for the cytotoxicity of the Pt-1C3 complex and of the anthraquinone moiety, both following a 4-h exposure to the DLD-1 cells. The 4-h exposure to Pt-1C3 produced cytotoxicity in 75% of the cell population at 20 μM, the maximum achievable concentration, whilst a 2-h exposure produced a marginally less pronounced reduction in cell number (Table 1). The extrapolated IC_{50} of Pt-1C3 was 11 ± 1 μM following a 4-h exposure and thus, the potency and extent of cell kill induced was greater than observed for cisplatin, but not significantly different to JM118 ($P < 0.05$, Table 1). The potency and extent of cytotoxicity was independent of exposure time and indicates that the compound, unlike cisplatin, achieved a rapid intracellular accumulation and distribution. However, the anthraquinone

($\lambda_{ex} = 488$ nm, 10–15% laser strength, $\lambda_{em} = 505$–530 nm). Panel (e) highlights localisation of Pt-1C3 ($\lambda_{ex} = 543$ nm, 76% laser strength, $\lambda_{em} > 560$ nm). Panel (f) is the overlay of panels (d and e). Panels (g–i) were obtained from cells incubated in the presence of Pt-1C3 (12 μM) for 4–5 h at 37 °C in the presence of the lysosomal stain LysoTracker Green (0.075 μM, 60 min, 37 °C). Panel (g) highlights localisation of the lysosomal stain ($\lambda_{ex} = 488$ nm, 10–15% laser strength, $\lambda_{em} = 505$–530 nm). Panel (h) highlights localisation of Pt-1C3 ($\lambda_{ex} = 543$ nm, 76% laser strength, $\lambda_{em} > 560$ nm). Panel (i) is the overlay of panels (g and h).

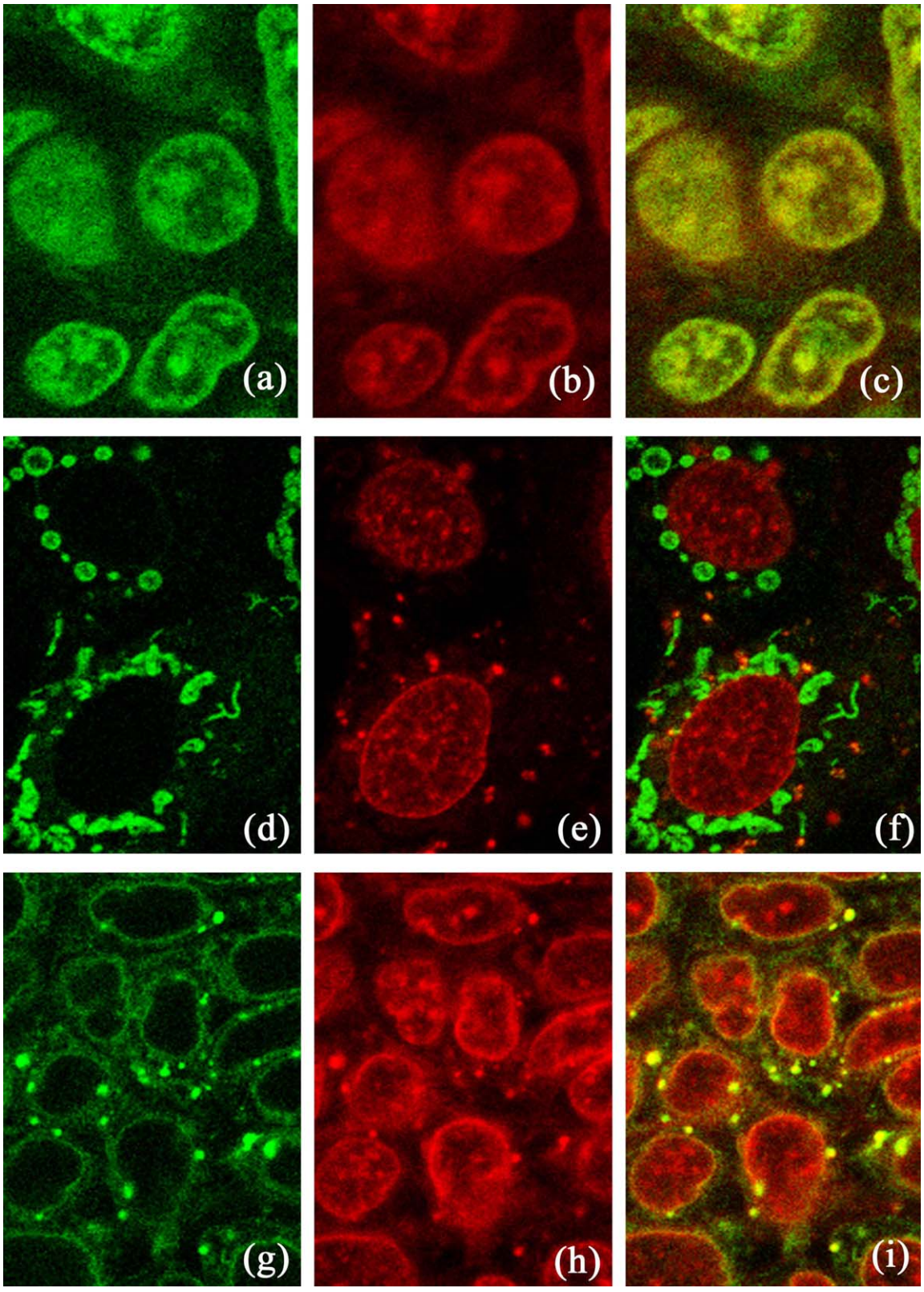

Fig. 4 – Cellular localisation of doxorubicin. DLD-1 cells were grown to 80% confluency on glass coverslips in 6-well tissue culture plates and drugs were localised using confocal fluorescence microscopy. Panels (a–c) were obtained from cells incubated in the presence of doxorubicin (12 μM) for 4–5 h at 37 °C in the presence of the cell permeant nuclear stain SYTO21 (5 μM, 2 h, 37 °C). Panel (a) highlights localisation of the nuclear stain (λ_{ex} = 488 nm, 10–15% laser strength, λ_{em} = 505–530 nm). Panel (b) highlights localisation of doxorubicin (λ_{ex} = 543 nm, 76% laser strength, λ_{em} > 560 nm). Panel (c) is the overlay of panels (a and b). Panels (d–f) were obtained from cells incubated in the presence of doxorubicin (12 μM) for 4–5 h at 37 °C in the presence of the mitochondrial stain MitoTracker Green (0.2 μM, 1 h, 37 °C). Panel (d) highlights

moiety on its own was also able to generate cytotoxicity in DLD-1 cells following either a 4 or a 2-h exposure (Fig. 2c and Table 1). At the highest possible concentration of 1C3 (i.e. 20 μM), the extent of cell kill was 52% and the extrapolated potency was 21 ± 6 μM for a 4-h exposure. Neither the potency nor the extent of cytotoxicity was significantly different than observed for the platinum containing anthraquinone. These results suggest that the nature of the cytotoxic effect may not be due to the platinum and is more likely to have been generated by the anthraquinone moiety.

3.2. Sub-cellular localisation of Pt-1C3 and 1C3

The possible lack of any platinum-dependent cytotoxicity could have resulted from a failure of the complex to accumulate within the nuclear compartment. The anthraquinone moiety displays fluorescent properties that enabled investigation of drug distribution using confocal fluorescence microscopy. The 1C3 moiety on its own showed no discernible difference in intracellular distribution compared to Pt-1C3. Thus only the intracellular distribution of Pt-1C3 is shown in Fig. 3 in comparison with fluorescent probes specific to defined organelles. For example, Fig. 3a shows that localisation of the probe SYTO21 was confined to the nuclear compartment. In contrast, the distribution of Pt-1C3 (Fig. 3b) was punctate, and as demonstrated by the overlay in Fig. 3c, distinct from the nuclear compartment. This indicates that the Pt-1C3 compound, whilst rapidly taken up by DLD-1 cells, did not enter the nucleus.

Two potential ''non-nuclear'' compartments in which the Pt-1C3 complex may accumulate are the mitochondria and lysosomes. Fig. 3d–f demonstrates the relative distributions of Pt-1C3 and the mitochondrial marker, MitoTracker Green. In particular, the overlay panel (Fig. 3f) indicates that the distributions for these two compounds were mutually exclusive. The sub-cellular distribution of the lysosomal probe, LysoTracker Green, also shows a punctate pattern (Fig. 3g). Moreover, inspection of the overlay in Fig. 3i indicates that the fluorescent dye and Pt-1C3 are similar—the yellow stain in the overlay is indicative of co-localisation. The distribution patterns displayed in Fig. 3 were obtained following 4-h incubation and there was no difference with a 1 or 2-h exposure to drug and fluorescent probe (data not shown). Fluorescence quenching of intercalators in the presence of DNA has been reported previously [25]. DNA titration experiments displayed minimal quenching of 1C3 or Pt-1C3 fluorescence in the presence of calf thymus DNA, with fluorescence intensity remaining above 60% of the initial peak intensity (data not shown). In addition, preliminary results indicate that the whole cell accumulation of Pt-1C3 is approximately five times higher than that of cisplatin (data not shown). The results suggest that the Pt-1C3 complex remains largely intact in the cells, within the lysosomes. Furthermore, atomic absorption spectroscopy failed to detect any platinum incorporated into DNA extracted from DLD-1 cells following drug exposure up to 24 h. Mislocalisation of Pt-1C3 to the lysosomes is therefore responsible for the lack of difference in cytotoxicity produced by the anthraquinone complexed platinum from that of the organic molecule per se. This suggests that the Pt-1C3 complex remains largely intact in the cells, within the lysosomes. Exactly the same sub-cellular distribution profile was observed for the 1C3 parent compound as for Pt1C3.

3.3. Sub-cellular localisation of doxorubicin

The distribution of the established anthraquinone containing anticancer agent, doxorubicin, was also examined in the DLD-1 cells to ascertain whether the lack of nuclear localisation of Pt-1C3 was a general feature of anthraquinones. Fig. 4a–c indicates that doxorubicin did in fact localise within the nuclear compartment of DLD-1 cells, which is in agreement with the potent and extensive cytotoxicity of this compound. There was no appreciable distribution of doxorubicin within either the mitochondrial (Fig. 4d–f) or lysosomal (Fig. 4g–i) compartments, the latter being in contrast to Pt-1C3.

4. Discussion

Cellular uptake of cisplatin has long been recognised as a limiting factor in the efficacy of this important clinical anticancer drug. The mechanism of uptake is not fully understood, but is likely to involve sparing trans-membrane diffusion [26] and a role for the copper import pump has also been implicated [27,28]. Once inside the cell cisplatin reaches the nuclear compartment and a great deal is known about the molecular interaction with DNA and the nature of the intra-strand cross-links formed [29]. However, the precise cellular distribution and the process by which cisplatin reaches the nucleus are yet to be elucidated. One of the factors precluding our understanding is the lack of simple analytical or imaging techniques for most platinum anticancer drugs. Fluorescently labelled cisplatin derivatives provide valuable information on cellular distribution [30,31], yet the similarity of these derivatives to the parent compound must be viewed with caution. Nonetheless, fluorescein [31], carboxyfluorescein [30] and Alexa Flour 546 [32] derivatives of cisplatin demonstrate the potential for sub-cellular sequestration of drugs in non-nuclear compartments, predominantly Golgi vesicles and lysosomes.

In an effort to more effectively generate platinum–DNA adducts, an alkyl–amino anthraquinone moiety was incorporated into a novel Pt(II)-complex. This strategy was to promote adequate cellular accumulation and nuclear localisation of the Pt(II)-complex by virtue of the hydrophobicity and DNA

localisation of the mitochondrial stain (λ_{ex} = 488 nm, 10–15% laser strength, λ_{em} = 505–530 nm). Panel (e) highlights localisation of doxorubicin (λ_{ex} = 543 nm, 76% laser strength, λ_{em} > 560 nm). Panel (f) is the overlay of panels (d and e). Panels (g–i) were obtained from cells incubated in the presence of doxorubicin (12 μM) for 4–5 h at 37 °C in the presence of the lysosomal stain LysoTracker Green (0.075 μM, 30 min, 37 °C). Panel (g) highlights localisation of the lysosomal stain (λ_{ex} = 488 nm, 10–15% laser strength, λ_{em} = 505–530 nm). Panel (h) highlights localisation of doxorubicin (λ_{ex} = 543 nm, 76% laser strength, λ_{em} > 560 nm). Panel (i) is the overlay of panels (g and h).

intercalating properties of the anthraquinone group. Anthracyclines are well established to intercalate with DNA [33] and many studies have shown that doxorubicin preferentially accumulates in the nuclear compartment of cells [34,35], likely due to the nuclear DNA sequestration of drug that comes into contact with it. The presence of the anthraquinone in the Pt-1C3 structure may generate also novel DNA adducts, thereby evading the DNA repair processes that limit platinum based chemotherapy. The cytotoxic potency of the Pt-1C3 compound was significantly higher compared to cisplatin and was similar to the 1C3 moiety per se. Further examination of the Pt-1C3 and 1C3 compounds indicated that both were rapidly and efficiently accumulated within the lysosomal compartment of the cells and that no platinum was observed in the nucleus. Lysosomal trapping of basic compounds, such as Pt-1C3, will contribute to reduced efficacy of the compound to produce DNA damage and resultant apoptosis.

The results in the present investigation clearly demonstrate that sequestration of the novel Pt-1C3 drug within lysosomes may limit its effectiveness as an anticancer drug. Both Pt-1C3 and 1C3 were localised to the lysosomes and displayed similar cytotoxicity profiles. The mechanism of Pt-1C3 cytotoxicity is unlikely to involve DNA damage as the results indicate that little, if any, of the compound reaches the cell nucleus. Thus, the toxicity was due to lysosomal accumulation, most probably leading to disruption. This phenomenon has previously been observed as a late development in the cascade of toxicity produced by cisplatin in renal cells [36] and neural ganglia [37]. Conversely, the accumulation of platinum complexes within lysosomes and other acidic compartments is a well-established detoxification mechanism [38] and has been implicated in mediating resistance to protonatable drugs such as daunorubicin [39,40]. The sequestration of drug away from the nucleus and thus preventing attainment of sufficient drug concentration at the target region is readily classified as a pharmacokinetic means of conferring resistance. There are two possible mechanisms to account for the accumulation of Pt-1C3 within the lysosomes. Firstly, the presence of a protonatable primary amine group will render the compound susceptible to pH-dependent accumulation within the highly acidic internal environment of lysosomes. Alternatively, the relative amphiphilicity of Pt-1C3 will enable rapid partitioning of the compound in the plasma membrane, but prevent diffusion through the bilayer core. Subsequent membrane internalisation will traffic Pt-1C3 to the lysosomal compartment via early and late endosomes. Regardless of the precise mechanism, the ultimate consequence is sequestration of the compound away from the nuclear compartment.

Several related, but dinuclear, anthraquinone–platinum complexes have also been synthesised with the aim of facilitating cytotoxic efficacy. These dinuclear platinum complexes produced a more potent cytotoxicity than cisplatin and displayed significant nuclear localisation in A2780 ovarian carcinoma cells [25]. However, in a resistant variant of the A2780 cells the complexes were rapidly accumulated in the acidic cellular compartments [41]. Interestingly, this sequestration was not apparent in a platinum resistant osteosarcoma cell line, which was characterised by rapid nuclear localisation of the dinuclear complexes [42]. The mononuclear Pt–anthraquinone complex used in the present investigation was associated with rapid intra-lysosomal sequestration in DLD-1 colon carcinoma cells. This may partly explain the lack of sensitivity exhibited by colon carcinoma to platinum based chemotherapy and highlights the need for extensive screening of potential new anticancer agents in numerous cell lines.

Future efforts to improve the intracellular fate of anthraquinone–platinum complexes will need to improve DNA targeting efficacy and evade the intra-lysosomal sequestration in order to generate cytotoxicity. Modification of the ''linker'' group and substitution within the anthracycline moiety may prove useful in ensuring that the drug reaches the nucleus.

Acknowledgements

This research was funded by a Cancer Research UK Program grant (SP1861/0401).

REFERENCES

[1] Skeel RT. Antineoplastic drugs and biologic response modifiers: classification, use and toxicity of clinically useful agents. In: Skeel RT, editor. Handbook of cancer chemotherapy. Lippincott Williams and Wilkins; 1999. p. 63–143.
[2] Andrews PA, Howell SB. Cellular pharmacology of cisplatin: perspectives on mechanisms of acquired resistance. Cancer Cells 1990;2(2):35–43.
[3] Harrap KR. Initiatives with platinum- and quinazoline-based antitumor molecules—Fourteenth Bruce F. Cain Memorial Award Lecture. Cancer Res 1995;55(13):2761–8.
[4] Niedner H, Christen R, Lin X, Kondo A, Howell SB. Identification of genes that mediate sensitivity to cisplatin. Mol Pharmacol 2001;60(6):1153–60.
[5] Hall MD, Failes TW, Hibbs DE, Hambley TW. Structural investigations of palladium(II) and platinum(II) complexes of salicylhydroxamic acid. Inorg Chem 2002;41(5):1223–8.
[6] Kelland LR, Sharp SY, O'Neill CF, Raynaud FI, Beale PJ, Judson IR. Mini-review: discovery and development of platinum complexes designed to circumvent cisplatin resistance. J Inorg Biochem 1999;77(1–2):111–5.
[7] Cvitkovic E. Ongoing and unsaid on oxaliplatin: the hope. Br J Cancer 1998;77(Suppl. 4):8–11.
[8] Temple MD, McFadyen WD, Holmes RJ, Denny WA, Murray V. Interaction of cisplatin and DNA-targeted 9-aminoacridine platinum complexes with DNA. Biochemistry 2000;39(18):5593–9.
[9] Gean KF, Ben-Shoshan R, Ramu A, Ringel I, Katzhendler J, Gibson D. Preparation, characterization and the anticancer activity of a novel series of triaminemonochloroplatinum(II) cations linked to anthraquinone intercalators. Eur J Med Chem 1991;26:593–8.
[10] Gibson D, Binyamin I, Haj M, Ringel I, Ramu A, Katzhendler J. Anthraquinone intercalators as carrier molecules for second-generation platinum anticancer drugs. Eur J Med Chem 1997;32:823–31.
[11] Gibson D, Gean KF, Ben-Shoshan R, Ramu A, Ringel I, Katzhendler J. Preparation, characterization, and anticancer activity of a series of *cis*-PtCl2 complexes linked to anthraquinone intercalators. J Med Chem 1991;34(1):414–20.
[12] Gibson D, Mansur N, Gean KF. Preparation, characterization, and antitumor properties of *cis*-PtCl2

complexes linked to anthraquinones through position number 2. J Inorg Biochem 1995;58(2):79–88.
[13] Kitov S, Ben-Shoshan R, Ringel I, Gibson D, Katzhendler J. The effect of cis-platin analogues derived from aminoalkylaminoanthraquinones on DNA cleavage: an electron microscopy study. Eur J Med Chem 1988;23: 381–3.
[14] Cheng CC, Zbinden G, Zee-Cheng RK. Comparison of antineoplastic activity of aminoethylaminoanthraquinones and anthracycline antibiotics. J Pharm Sci 1979;68(3):393–6.
[15] Murdock KC, Child RG, Fabio PF, Angier RB, Wallace RE, Durr FE, et al. Antitumor agents. 1. 1,4-Bis[(aminoalkyl)amino]-anthracene-9,10-diones. J Med Chem 1979;22(9):1024–30.
[16] Denny WA, Wakelin LP. Kinetics of the binding of mitoxantrone, ametantrone and analogues to DNA: relationship with binding mode and anti-tumour activity. Anticancer Drug Des 1990;5(2):189–200.
[17] Islam SA, Neidle S, Gandecha BM, Partridge M, Patterson LH, Brown JR. Comparative computer graphics and solution studies of the DNA interaction of substituted anthraquinones based on doxorubicin and mitoxantrone. J Med Chem 1985;28(7):857–64.
[18] Lown JW, Morgan AR, Yen SF, Wang YH, Wilson WD. Characteristics of the binding of the anticancer agents mitoxantrone and ametantrone and related structures to deoxyribonucleic acids. Biochemistry 1985;24(15):4028–35.
[19] Smith PJ, Desnoyers R, Blunt N, Giles Y, Patterson LH, Watson JV. Flow cytometric analysis and confocal imaging of anticancer alkylaminoanthraquinones and their N-oxides in intact human cells using 647-nm krypton laser excitation. Cytometry 1997;27(1):43–53.
[20] Barasch D, Zipori O, Ringel I, Ginsburg I, Samuni A, Katzhendler J. Novel anthraquinone derivatives with redox-active functional groups capable of producing free radicals by metabolism: are free radicals essential for cytotoxicity? Eur J Med Chem 1999;34(7–8):597–615.
[21] Cai L, Lim K, Ren S, Cadena RS, Beck WT. Synthesis and in vitro antitumor activity of oligonucleotide-tethered and related platinum complexes. J Med Chem 2001;44(18):2959–65.
[22] De Lean A, Munson PJ, Rodbard D. Simultaneous analysis of families of sigmoidal curves: applications to bioassay, radioligand assay, and physiological dose–response curves. Am J Physiol 1978;235:E97–102.
[23] Platts JA, Hibbs DE, Hambley TW, Hall MD. Calculation of the hydrophobicity of platinum drugs. J Med Chem 2001;44(3):472–4.
[24] Hall MD, Martin C, Ferguson DJP, Phillips RM, Hambley TW, Callaghan R. Comparative efficacy of novel platinum(IV) compounds with established chemotherapeutic drugs in solid tumour models. Biochem Pharmacol 2004;67:17–30.
[25] Jansen BA, Wielaard P, Kalayda GV, Ferrari M, Molenaar C, Tanke HJ, et al. Dinuclear platinum complexes with *N*,*N*′-bis(aminoalkyl)-1,4-diaminoanthraquinones as linking ligands. Part I. Synthesis, cytotoxicity, and cellular studies in A2780 human ovarian carcinoma cells. J Biol Inorg Chem 2004;9(4):403–13.
[26] Gately DP, Howell SB. Cellular accumulation of the anticancer agent cisplatin: a review. Br J Cancer 1993;67(6):1171–6.
[27] Ishida S, Lee J, Thiele DJ, Herskowitz I. Uptake of the anticancer drug cisplatin mediated by the copper transporter Ctr1 in yeast and mammals. Proc Natl Acad Sci USA 2002;99(22):14298–302.
[28] Lin X, Okuda T, Holzer A, Howell SB. The copper transporter CTR1 regulates cisplatin uptake in *Saccharomyces cerevisiae*. Mol Pharmacol 2002;62(5):1154–9.
[29] Jamieson ER, Lippard SJ, Structure. Recognition, and processing of cisplatin–DNA adducts. Chem Rev 1999;99(9):2467–98.
[30] Molenaar C, Teuben JM, Heetebrij RJ, Tanke HJ, Reedijk J. New insights in the cellular processing of platinum antitumor compounds, using fluorophore-labeled platinum complexes and digital fluorescence microscopy. J Biol Inorg Chem 2000;5(5):655–65.
[31] Safaei R, Katano K, Larson BJ, Samimi G, Holzer AK, Naerdemann W, et al. Intracellular localization and trafficking of fluorescein-labeled cisplatin in human ovarian carcinoma cells. Clin Cancer Res 2005;11(2 Pt 1):756–67.
[32] Liang XJ, Shen DW, Chen KG, Wincovitch SM, Garfield SH, Gottesman MM. Trafficking and localization of platinum complexes in cisplatin-resistant cell lines monitored by fluorescence-labeled platinum. J Cell Physiol 2005;202(3):635–41.
[33] Gabbay EJ, Grier D, Fingerle RE, Reimer R, Levy R, Pearce SW, et al. Interaction specificity of the anthracyclines with deoxyribonucleic acid. Biochemistry 1976;15(10):2062–70.
[34] Coley HM, Amos WB, Twentyman PR, Workman P. Examination by laser scanning confocal fluorescence imaging microscopy of the subcellular localisation of anthracyclines in parent and multidrug resistant cell lines. Br J Cancer 1993;67(6):1316–23.
[35] Marquardt D, Center MS. Drug transport mechanisms in HL60 cells isolated for resistance to adriamycin: evidence for nuclear drug accumulation and redistribution in resistant cells. Cancer Res 1992;52(11):3157–63.
[36] Leibbrandt ME, Wolfgang GH, Metz AL, Ozobia AA, Haskins JR. Critical subcellular targets of cisplatin and related platinum analogs in rat renal proximal tubule cells. Kidney Int 1995;48(3):761–70.
[37] Stacchiotti A, Rezzani R, Rodella L, Ventura RG. Lysosomal changes in rat spinal ganglia neurons after prolonged treatment with cisplatin. Acta Anat (Basel) 1995;153(3): 236–42.
[38] Aggarwal SK. A histochemical approach to the mechanism of action of cisplatin and its analogues. J Histochem Cytochem 1993;41(7):1053–73.
[39] Bour-Dill C, Gramain MP, Merlin JL, Marchal S, Guillemin F. Determination of intracellular organelles implicated in daunorubicin cytoplasmic sequestration in multidrug-resistant MCF-7 cells using fluorescence microscopy image analysis. Cytometry 2000;39(1):16–25.
[40] Gong Y, Duvvuri M, Krise JP. Separate roles for the Golgi apparatus and lysosomes in the sequestration of drugs in the multidrug-resistant human leukemic cell line HL-60. J Biol Chem 2003;278(50):50234–9.
[41] Kalayda GV, Jansen BA, Molenaar C, Wielaard P, Tanke HJ, Reedijk J. Dinuclear platinum complexes with *N*,*N*′-bis(aminoalkyl)-1,4-diaminoanthraquinones as linking ligands. Part II. Cellular processing in A2780 cisplatin-resistant human ovarian carcinoma cells: new insights into the mechanism of resistance. J Biol Inorg Chem 2004;9(4):414–22.
[42] Kalayda GV, Jansen BA, Wielaard P, Tanke HJ, Reedijk J. Dinuclear platinum anticancer complexes with fluorescent *N*,*N*′-bis(aminoalkyl)-1,4-diaminoanthraquinones: cellular processing in two cisplatin-resistant cell lines reflects the differences in their resistance profiles. J Biol Inorg Chem 2005;10(3):305–15.